RSC Advances

PAPER

View Article Online
View Journal | View Issue

Cite this: *RSC Adv.*, 2014, **4**, 51926

Efficient and scalable synthesis of quantum dots using hexane as the solvent in a non-microfluidic flow reactor system†

Hong-Jie Yang and Hsing-Yu Tuan*

Quantum dots (QDs) synthesis has been widely carried out in Schlenk line systems. However, there are two drawbacks of these systems, which have restricted their use for large scale or commercial production of QDs. One is the use of expensive and high-boiling point solvents and the other is that QDs need to be continuously produced with high production rate to reduce production costs. Nowadays, microfluidic flow systems are the most popularly used systems for the continuous production of QDs. However, their narrow channels limit the reaction volume and flow rate. In this report, a non-microfluidic flow reactor system has been developed to synthesize high quality CdSe QDs by injecting the solution containing the mixture of Cd–oleic acid (Cd–OA) and Se–tributylphosphine (Se–TBP) into near critical or supercritical hexane. The optical properties of the produced CdSe QDs can be fine-tuned to almost cover the entire visible region (450–630 nm) by changing the reaction parameters. The CdSe QDs produced with this approach are similar to those produced in Schlenk line, and can be functionalized with a ZnS shell to enhance PL efficiency. Moreover, we have also achieved a continuous synthesis of 5 g CdSe QDs with a production rate of 2.5 g h^{-1} to demonstrate the potential capability of mass production with this system. White light emitting diodes can be prepared by using CdSe QDs as the phosphor dye. Finally, other types of QDs, such as CdS, ZnS, and ZnSe, were also synthesized to demonstrate the generalization of the developed approach.

Received 3rd June 2014
Accepted 15th September 2014

DOI: 10.1039/c4ra05279j

www.rsc.org/advances

Introduction

Colloidal fluorescing QDs exhibit unique, size-dependent physical and chemical properties compared to bulk materials, and can self-assemble into supercrystals if their size distribution is uniform.[1–6] These special properties have lead to the application of QDs in many fields such as optoelectronic devices, luminescent biological labels, and solar cells.[7–12] In accordance with their size-dependent properties, the synthesis of monodisperse QDs with uniform shape and size is an important key to obtain pure size-related properties that can be applied in diverse fields.[13,14] In 1993, an article about synthesizing nearly monodisperse cadmium chalcogenide nanoparticles by rapid injection of organometallic reagents into a hot coordinating solvent was made by Bawendi *et al.*, which implied that high quality monodisperse QDs could be easily produced in solution phase.[15] Subsequently, safer methods have been developed. For example, Peng *et al.* showed that high quality CdSe QDs can be generated without any size-selection by replacing the extremely toxic and pyrophoric precursor $Cd(CH_3)_2$ to a stable and less toxic chemical CdO.[16] Nowadays, a variety of synthetic approaches are available for the synthesis of monodisperse QDs in high quality *via* different types of precursors, ligands or solvents though different synthetic strategies such as hot injection, heating, microfluidic or microwave-assisted processes.[17–27]

Among the various synthetic routes, hot injection and non-injection methods are the most successful and commonly used methods for the preparation of highly luminescent colloidal QDs with controllable size, shape, and surface passivation.[28,29] However, the major drawbacks of these methods are the use of large amounts of expensive and high boiling point solvents, limited reaction temperature, unpredictable transport phenomena (hot injection), and difficulty in scaling-up the synthesis process.[30–32] Therefore, the development of a greener method having the potential for scale up, and utilizing cheaper, less toxic chemicals and reaction medium (solvents) to synthesize QDs is desirable.

Usually, high molecular weight solvents with high boiling point (trioctylphosphine oxide or octadecene) have been used to synthesize QDs. One way for using low molecular weight solvents with low boiling point is to conduct experiments at high pressure.[33] In addition, the reaction media can enhance their ability of solvating chemical compounds under sufficiently

Department of Chemical Engineering, National Tsing Hua University, 101, Section 2, Kuang-Fu Road, Hsinchu, Taiwan 30013, Republic of China. E-mail: hytuan@che.nthu.edu.tw; Fax: +886-3-571-5408; Tel: +886-3-572-3661

† Electronic supplementary information (ESI) available: UV-vis absorption and PL spectra of CdSe QDs. See DOI: 10.1039/c4ra05279j

high pressure. The physicochemical properties (density, viscosity, dielectric constant) of near critical and supercritical fluids can also be tuned by varying the pressure and temperature of the system, which have been considered to be environmentally benign solvents.[34] To date, research about the synthesis of nanomaterials under supercritical water and supercritical ethanol has been reported.[35–38] However, metal oxide nanoparticles, such as Fe_2O_3, TiO_2, CuO, ZnO, are easy to produce due to the oxidizing environment provided by supercritical water, making the synthesis of metals or non oxide based compound semiconductor difficult.[39] In addition, several commonly used precursors and organic ligands may be incompatible with water or ethanol; thus, using low molecular weight and more hydrophobic organic solvents may be a way to overcome these problems. A study using a microfluidic reactor for synthesizing CdSe QDs by Marre *et al.* has proven that adopting a supercritical fluid as the solvent is compatible with currently used chemicals and the results are superior to the conventional solvent (squalane).[33] However, the narrow pipeline and the micro-size reaction restrict the production rate. Therefore, the improvement of the synthesis of CdSe QDs using supercritical fluid technologies is desirable.

Here, we show a green and generalized approach for the synthesis of several types of colloidal fluorescing QDs. We use hexane which is a more environmentally friendly solvent than those previously used in hot injection methods. In addition, hexane is also a common industrial solvent, which implied that the cost of synthesizing QDs can be reduced. Using CdSe as an example, monodisperse CdSe QDs can be generated under near critical and supercritical hexane fluids, and their size can be fine tuned by changing the reaction temperature time. In addition, we improved the optical properties of CdSe QDs by coating ZnS shells to the surface of CdSe QDs, which has been a well-known tool to significantly enhance the quantum yield (QY) of CdSe QDs. Moreover, we use CdSe QDs as phosphors to prepare white light emitting diodes. To show the ability for the mass production of QDs in our system, we demonstrate the continuous synthesis of large scale CdSe QDs under supercritical hexane. Compared to a microfluidic reactor, our system possesses relatively high production rate due to the larger size of pipeline and reaction volume. The implementation of synthesizing CdSe QDs in flow reactor can offer several advantages over conventional methods, *e.g.*, batch reactor, in terms of time and cost. Finally, we prove the general applicability of our system by producing several types of colloidal fluorescing QDs, including CdS, ZnS, and ZnSe QDs.

Experimental section

Chemicals

Anhydrous hexane (95%), hexane (99.9%), toluene (99.9%), absolute ethanol, (99.8%), methanol (99.9%), hexadecylamine (98%), octadecene (90%), tributylphosphine (TBP, 97%), polymethyl methacrylate (PMMA, average Mw ~996 000), oleic acid (OA, 90%), chlorobenzene (99.5%), cadmium oxide (CdO, 99%), diethylzinc solution (1 M in hexane), hexamethyldisilathiane ($(TMS)_2S$), rhodamine 6G, sulfur (S, 99.5%), and selenium (Se, 99.5%) powder were purchased from Aldrich and were used without further purification. The Cd–OA solution (1 M) was prepared by heating 15 mL OA with 1.926 g CdO to 200 °C until a clear, light yellow solution was formed. The solution was further stored in a glove box. A 1 M stock solution of Se–TBP was prepared by dissolving 0.7896 g Se in 10 mL TBP at 150 °C until a clear, colorless solution was formed and further stored in a glove box.

Synthesis of CdSe QDs by supercritical equipment

CdSe QD reactions were carried out in a 10 mL stainless steel reactor similar to the apparatus used in previous reports.[40,41] The inlet of a stainless steel (1/16″ i.d.) tube was connected to an injector valve (Valco) coupled with a 0.5 mL injection loop. The temperature of the reactor was controlled by a temperature controller and maintained by heating and insulation tapes that covered the entire stainless steel reactor. A high-pressure liquid chromatography (HPLC) pump (Lab Alliance, series 1500) was used as a liquid delivering pump to transport organic liquid to pressurize the reactor system, and the system pressure was monitored by a digital pressure gauge. The reaction solution was prepared in a glove box by the addition of 0.35 mL 1 M Cd–OA and 0.35 mL 1 M Se–TBP into 0.3 mL anhydrous hexane and then loaded into a syringe.

In a typical reaction, the stainless steel reactor was heated to the reaction temperature and pressurized to 800 psi. The reaction solution was taken from the glove box and injected into a 0.5 mL sample loop. Next, the HPLC pump was turned on with an injection rate of 8 mL min^{-1} for 10 s and then turned off. The stainless steel reactor was quickly cooled by an ice-water bath when the reaction ended. The products were removed from the reactor and purified by the addition of 10 mL toluene and 20 mL ethanol, and then centrifuged at 8000 rpm for 5 min. The washing processes were repeated at least twice. The size control of CdSe QDs was achieved by varying the reaction temperature and time. For example, at a reaction temperature of 200 °C, the diameters of 2.45 nm and 2.94 nm QDs can be generated under reaction times of 30 s and 5 min, respectively. Under the same reaction time of 30 s, QDs with diameters of 2.45 nm and 2.73 nm can be produced at reaction temperatures of 200 °C and 270 °C, respectively (Fig. S1†).

Coating CdSe QDs with a ZnS shell

CdSe@ZnS QDs were prepared using a Schlenk line system. A reaction mixture containing 3.4 mL TBP, 0.3 mL diethylzinc solution, and 63 μL $(TMS)_2S$ was prepared in a glove box and then loaded into a syringe. A reaction flask containing 9 mg CdSe QDs, 1.5 g hexadecylamine, and 2.5 mL octadecene was evacuated at 100 °C for 1 h and then heated to 160 °C under an atmosphere of Ar. The Zn and S precursors were added dropwise to the stirring reaction flask using a syringe and a syringe pump. The injection process was divided into three stages at ~10 s intervals (one injection with three different injection rate). Each stage has the same heating rate (1 °C min^{-1}) and injection time (10 min) but different injection rates. For stage one, two, and three, the injection rates were 3.12 mL h^{-1},

4.62 mL h^{-1}, and 6.6 mL h^{-1}, respectively (Table 1). After the injection, the temperature of the reaction flask was decreased from 190 °C to 120 °C and reacted for 90 min. Finally, the products were purified by adding 10 mL toluene and 20 mL ethanol, and then centrifuged at 8000 rpm for 10 min. The washing processes were repeated at least twice.

Synthesis of other QDs (CdS, ZnS, and ZnSe) by supercritical equipment

The reaction procedure and purified processes were similar to the CdSe QDs reactions, except the precursor concentration, reaction time and reaction temperature. Cd–OA solution (1 M), Se–TBP solution (3 M), diethylzinc solution (1 M), and S–TBP solution (3 M) were used as the Cd, Se, Zn, and S precursors respectively. For the synthesis of CdS QDs, the reaction mixtures were composed of 0.2 mL Cd–OA, 67 μL S–TBP and 0.7 mL anhydrous hexane with a reaction time of 3 min and a reaction temperature of 240 °C. For the synthesis of ZnS QDs, the reaction mixtures were composed of 0.33 mL diethylzinc solution and 0.66 mL S–TBP with a reaction time of 5 min and a reaction temperature of 300 °C. For the synthesis of ZnSe QDs, the reaction mixtures were composed of 0.56 mL diethylzinc solution and 187 μL S–TBP with a reaction time of 5 min and a reaction temperature of 280 °C.

Scale up of CdSe QDs

A 10 mL continuous reactor made of stainless steel was used for the gram scale production of CdSe QDs. The inlet and outlet of the stainless steel reactor were both connected to a stainless steel (1/8″ i.d.) tube *via* a LM-6 HIP (High Pressure Equipment Co.) reducer. The inlet of the reactor was connected to a six-way valve (Valco) containing a 10 mL injection loop *via* a stainless steel (1/8″ i.d.) tube and the outlet of the reactor was connected to a micro control-metering valve (HF4-V, HIP) *via* a stainless steel (1/8″ i.d.) tube.

In continuous reaction for the production of 5 g CdSe QDs, the reactor was heated to 300 °C and then pressurized to 1000 psi. A syringe containing 5.4 mL Cd–OA (1 M), 1.8 mL Se–TBP (3 M), and 2.8 mL anhydrous hexane prepared in a glove box was taken from the glove box and injected into the a 10 mL sample loop. Next, the HPLC pump was turned on with an injection rate of 1 min mL^{-1}, and then slowly the micro control-metering valve was opened to maintain the system pressure (~1000 psi). A flask was placed at the outlet of the micro control-metering valve to collect the products. After 20 min reaction time, another reaction solution was prepared and injected into the 10 mL sample loop. The injection procedure was repeated six times with total reaction volume of 60 mL and total reaction time of 2 h. The collected products were purified by the addition of ethanol and then centrifuged at 8000 rpm for 8 min. The washing processes were repeated at least twice.

Fabrication of white light emitting diodes (LEDs)

CdSe QDs and PMMA mixtures were prepared by the addition of 50 mg PMMA into a CdSe QDs solution (5 mg in 1 mL chlorobenzene) and then vigorously stirring for 10 h at room temperature. White LEDs were fabricated by coating the mixtures on a surface mounted device (SMD) type of blue emission LED with chip size 5 mm × 5 mm and an emission peak at 460 nm. After coating, the solvent was dried in a vacuum oven at 70 °C for 60 min.

Characterization

The purified QDs were dispersed in hexane for UV-vis absorbance and fluorescence spectra measurements. To obtain accurate QY, the optical density at the first absorption peak of the QDs and absorption peak of the dye were set to a similar value, both below 0.1 to avoid any reabsorption. PL measurement was carried out immediately after the UV-vis absorbance measurement. The QY of the QDs was calculated using a methanol solution of Rhodamine 6G as a standard (QY = 0.95) based on the equation from published articles.[42] UV-vis spectra and fluorescence spectra were recorded on a Hitachi U-4100 spectrophotometer and a Hitachi F-2500 fluorescence spectrophotometer with an excitation wavelength of 410 nm. Transmission electron microscopy (TEM) images and selected area electron diffraction (SAED) patterns were obtained on a JEM 2100F and a FEI-TEM, Philips Technai at an acceleration voltage of 200 kV. X-ray diffraction (XRD) patterns were measured on a Rigaku, Ultima IV X-ray diffractometer using Cu Kα radiation. X-ray photoelectron spectroscopy (XPS) measurements were taken on a PHI Quantera SXM using a focused monochromatic Al X-ray (1486.6 eV) source. Fourier transform infrared (FTIR) spectra were recorded by mixing a given sample in a KBr pellet and using a Perkin-Elmer Spectrum RXI FTIR spectrometer with 32 scans.

Table 1 Injection parameters of the coating process

	Stage 1	Stage 2	Stage 3
Heating rate	1 °C min^{-1}	1 °C min^{-1}	1 °C min^{-1}
Injection time	10 min	10 min	10 min
Injection rate	3.12 mL h^{-1}	4.62 mL h^{-1}	6.6 mL h^{-1}
Injection amount	0.52 mL	0.77 mL	1.1 mL
Reaction temperature	160 °C to 170 °C	170 °C to 180 °C	180 °C to 190 °C

Results and discussions

Solvents definitely have a very important impact on the environment in many chemical industries.[43] For synthesis of nanomaterials in solution phase, the amount of solvent used is always much higher than precursors or ligands. Therefore, using greener solvents and also common industrial solvents is a crucial step to quantify the production even toward industrialization. In our system, the simple alkane solvent, hexane (the physical properties of hexane are shown in Fig. 1a), was chosen due to several advantages. First, hexane is a commonly available and inexpensive industrial solvent. Second, previous literature has indicated that hexane has high environmental credits (according to energy recovery and environmental impacts on the production of hexane), which indicates that hexane is a greener solvent than the commonly used solvent (trioctylphosphine oxide or octadecene) for the synthesis of CdSe QDs.[44] Third, the reaction parameter should be easier to manipulate when the synthesis is conducted under a non-coordinating solvent.

Fig. 1b shows a schematic picture of QDs synthesized under high pressure hexane. In a typical reaction, colloidal CdSe QDs were produced by the decomposition of Cd–OA and Se–TBP under near critical or supercritical hexane. Fig. 2 and Fig. 3 show the representative analysis results (TEM, HRTEM, XRD, optical measurement, and FTIR) of CdSe QDs produced by the decomposition of reaction mixtures containing 0.35 mL Cd–OA (1 M), 0.35 mL Se–TBP (1 M), and 0.3 mL hexane and synthesizing at 270 °C for 5 min. TEM images (Fig. 2) confirm the dot shape of the products with an average diameter of about 2.95 nm without any size selection. These dot shaped nanoparticles tend to self-assemble into close-packed two-dimensional arrays on the TEM grid, which indicates the monodispersity of the obtained product (Fig. 2a and b). From the fast Fourier transform spectra of the two-dimensional array nanoparticles (Fig. 2a inset), the pattern is consistent with a face centred cubic superlattice. HRTEM images (Fig. 2e and f) show distinct lattice planes, showing high crystallinity of the nanoparticles. The crystalline structure of the synthesized nanoparticles was investigated by XRD. Fig. 3b shows the XRD pattern of the CdSe QDs. The diffraction peaks correspond to the zinc blend and wurtzite structure of CdSe, which may be a combination of wurtzite structure with zinc blend stacking faults.[45] Broad peaks in the XRD pattern indicate a small crystal with an average size of ~2.9 nm calculated from the Scherrer equation. The size is in close agreement with the nanoparticle size obtained from the TEM images (Fig. 2).[46] The optical properties (absorption and PL spectra) of the as-synthesized CdSe QDs are shown in Fig. 3a. The first absorption and PL maxima are about 551 nm and 566 nm (15 nm Stokes shift), respectively. QY of the as-synthesized CdSe QDs is about 15%. The sharp peak in the absorption spectra and the narrow full-width half-maximum value in the PL spectra (32 nm) further indicate the narrow size distribution of the as-synthesized CdSe QDs. In addition, the average diameters of CdSe QDs can be calculated from first absorption peak in the UV-vis spectra. The calculated value is about 3 nm, which is very close to the results obtained from the XRD pattern (Fig. 3b) and the TEM images (Fig. 2).[47]

The CdSe QDs synthesized by our supercritical equipment can be easily dispersed in most organic solvents. Intuitively, the OA and TBP should be surface ligands on the CdSe QDs because hexane is a non-coordinating solvent. To confirm this hypothesis and understand the surface state of the as-synthesized CdSe QDs, FTIR and XPS were performed. Fig. 3c shows the FTIR spectra of OA, TBP, and the as-synthesized CdSe QDs. For liquid OA, the carboxylic acid group would generate O–H stretch (broad peak between 3500 and 2500 cm^{-1}), in plane O–H stretch (1466 cm^{-1}), C=O stretch (1711 cm^{-1}), and C–O stretch (1285 cm^{-1}), and the remaining peaks at 2850 cm^{-1}, 2920 cm^{-1}, and 3005 cm^{-1} were attributed to the symmetric CH_2 stretch, the asymmetric CH_2 stretch, and the C–H stretch in C=C–H, respectively.[48] For pure TBP, C–P stretch (appeared at 1300 cm^{-1} to 1000 cm^{-1}), symmetric CH_2 stretch (2870 cm^{-1}), asymmetric CH_2 stretch (2925 cm^{-1}), asymmetric in-plane (1463 cm^{-1}), and symmetric rocking mode (1376 cm^{-1}) of CH_3 group were detected.[49] In comparison with the FTIR spectra of liquid OA and pure TBP, we can measure the symmetric CH_2 stretch (2872 cm^{-1}) and the asymmetric CH_2 stretch (2923 cm^{-1}) both contributed from OA and TBP, C–P stretch (1030 cm^{-1} and 1080 cm^{-1}) assigned to TBP, and C–H stretch in C=C–H (3030 cm^{-1}) generated by OA. It is worth noting that the C=O stretch (1711 cm^{-1}) in the IR spectra of pure OA disappeared in the IR spectra of the as-synthesized CdSe QDs. Instead, a new band at about 1500 cm^{-1} was assigned to the COO^- asymmetric vibration, and the COO^- symmetric vibration may overlap with the asymmetric in-plane or symmetric rocking mode of CH_3 group.[50] In

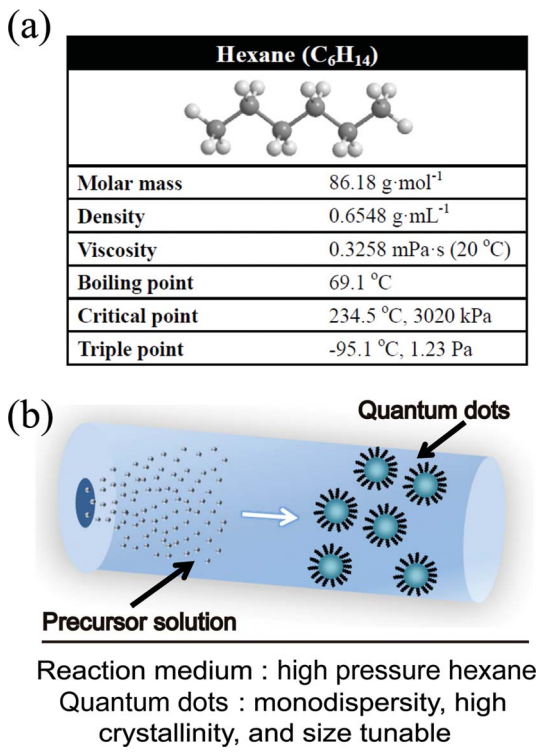

Fig. 1 (a) The physical properties of hexane. (b) Schematic picture of QDs synthesized under high pressure hexane.

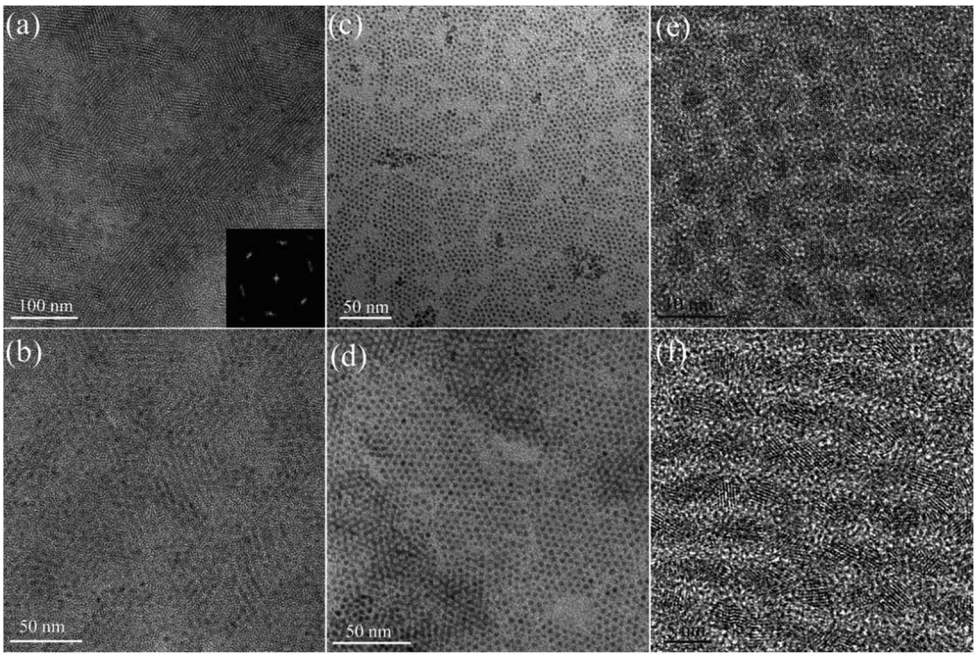

Fig. 2 (a and b) TEM images of the CdSe QDs in dense regions, the inset is the corresponding fast Fourier transform. (c and d) TEM images of the CdSe QDs in relatively sparse areas. (e and f) HRTEM images of the CdSe QDs. The analyzed CdSe QDs were obtained by the decomposition of Cd–OA with Se–TBP under supercritical hexane and synthesizing at 270 °C for 5 min.

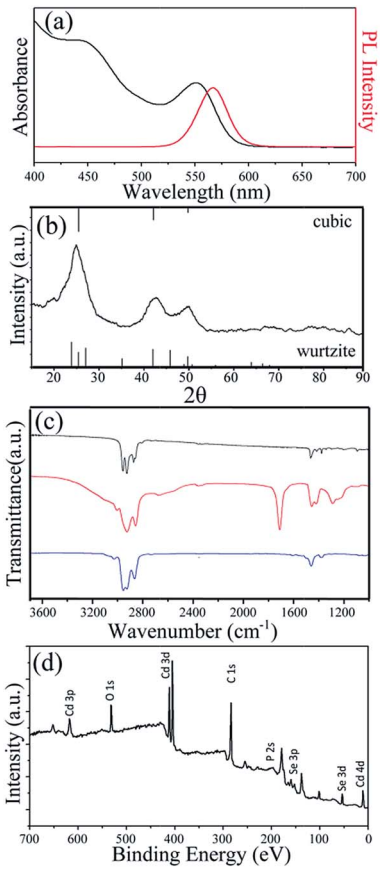

Fig. 3 (a) UV-vis absorption, PL spectra, and (b) XRD pattern of the as-synthesized CdSe QDs. (c) FTIR spectra of pure TBP (black), liquid OA (red), and CdSe QDs (blue) obtained from the decomposition of Cd–OA with Se–TBP. (d) XPS survey spectra of CdSe QDs.

addition, P can also be detected in the XPS full spectrum (Fig. 3d), which indicates that the TBP indeed exists on the CdSe QDs surface. According to the analysis results based on FTIR and XPS, the surface of the CdSe QDs was passivated by OA (from Cd–OA) and TBP (from Se–TBP). In some studies, OA and TBP have been shown as stabilizers to coordinate the nucleation and growth of nanocrystals in the growth process. We believe that OA and TBP play the same roles in our system.[51,52]

The QY of the CdSe QDs synthesized by our synthetic route is about 15% (Fig. 3a). The QY is sensitive to the surface properties of the QDs such as surface ligands or dispersion medium (solvent).[53,54] Numerous methods have been developed to improve the QY of the QDs such as organic or inorganic passivation.[55] Obviously, inorganic passivation is superior to organic passivation. For now, the most used method is the ZnS passivation approach, which is an effective method that can separate the core from the surrounding medium to prevent the

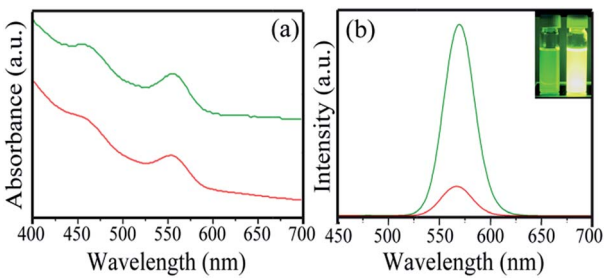

Fig. 4 (a) UV-vis absorption and (b) PL spectra of CdSe QDs (red) and CdSe QDs coating with ZnS shells (green). The images of CdSe QDs and CdSe@ZnS QDs under UV excitation are also shown in the inset.

photo-oxidation and stabilize the surface. Therefore, ZnS passivation of CdSe QDs was performed. Fig. 4 shows the absorption and PL spectra of CdSe QDs and CdSe@ZnS QDs. There is a small red shift in UV-vis absorption spectrum (4 nm) and PL spectrum (4 nm), which is a common phenomenon after coating ZnS shell. We can see that the QY is significantly enhanced by simply comparing the intensity of the PL peaks and the digital photos in the inset (the optical density at the first absorption peak and the concentration of the CdSe QDs and CdSe@ZnS QDs solutions were set to a similar value). The calculated QY of CdSe@ZnS QDs is 65%, which is significantly enhanced compared to the raw materials, CdSe QDs (15%).

Next, we tested the ability of the supercritical equipment to control the size of the CdSe QDs by varying reaction parameters. We observed that the size of the CdSe QDs can simply be regulated by changing the growth time and reaction temperature (Fig. S1†). By varying these two reaction parameters, a series of absorption and PL spectra of CdSe QDs synthesized with particle sizes ranging from approximately 2.01 nm to 5.61 nm (calculated from absorption spectra, Fig. 5a), emission wavelengths ranging from 450 nm to 630 nm (covering almost the entire visible region, Fig. 5b), QY of about 5–15%, and color ranging from green to red were obtained (Fig. 5a inset). The TEM images of three CdSe QDs samples with average diameters of about 2.2 nm (Fig. 6a), 2.9 nm (Fig. 6b), and 4.0 nm (Fig. 6c) demonstrate that the size of CdSe QDs can be controlled by manipulating the reaction conditions. According to the experimental results, large size CdSe QDs tend to form at high reaction temperature and long growth time. For example, at the same growth time of 5 min reaction time, CdSe QDs with 3 nm and 3.51 nm size were generated at 270 °C and 330 °C, respectively. At the same growth temperature of 270 °C, CdSe QDs with 2.6 nm and 3 nm size were produced with the growth time of 1 and 5 min, respectively. This trend is consistent with many published literature.[56,57]

Using continuous reactor to perform chemical synthesis is an efficient way to lower production costs. Compared with conventional batch reactor, continuous reactor has many advantages such as safety, low cost, and both time and space saving.[58,59] A well-known continuous reactor, microfluidic reactor, has shown their ability to generate several types of QDs with controllable size and shape.[60,61] However, two drawbacks inside the narrow channels makes us reconsider its feasibility. First, the narrow channels confine the volume flow rate, which indicates the difficulty of scale up. Second, the system tends to block if nanocrystals or other insoluble materials precipitate. Supercritical fluid equipment had been demonstrated in the continuous synthesis of Ge and Si nanowires in the past.[62] In this article, we also show the ability to scale up using this supercritical fluid equipment by performing continuously producing 5 g CdSe QDs with a production rate of about ~2.5 g h^{-1}. The schematic picture of our continuous flow system is shown in Fig. 7a. The digital image of the 5 g CdSe QDs produced by this system is shown in Fig. 7b, and Fig. 7c shows the 5 g CdSe QDs irradiated by UV lamp. Fig. 7d also shows a digital image of the 5 g CdSe QDs dispersed in hexane. These results show that the mass production of CeSe QDs by our

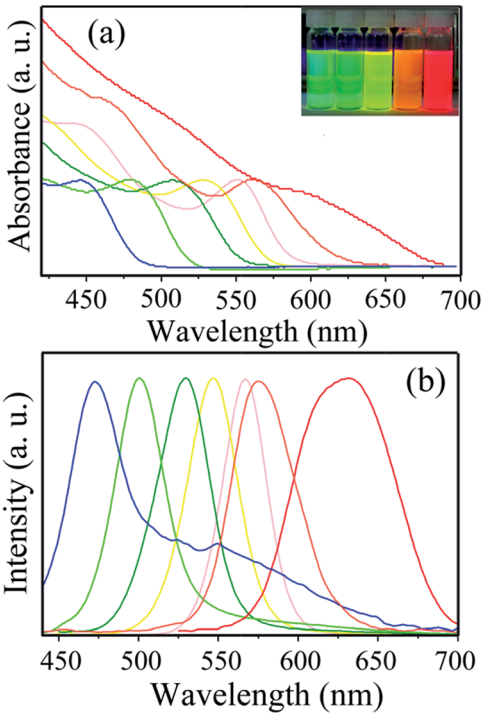

Fig. 5 (a) UV-vis absorption and (b) PL spectra of the CdSe QDs with sizes ranging from approximately 2.01 nm to 5.61 nm obtained by varying reaction temperature and growth time. The inset shows a photography of CdSe QDs irradiated by a UV lamp with color ranging from green to red.

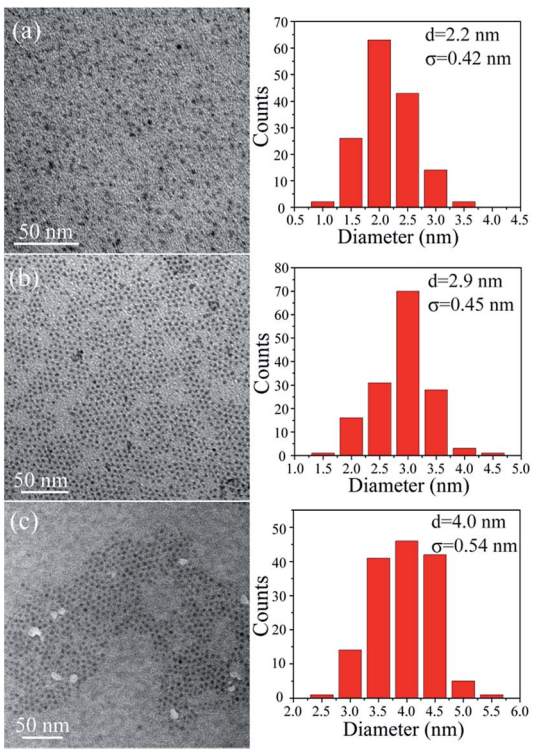

Fig. 6 (a–c) TEM images and size distribution histogram of three CdSe QDs samples with average diameter and standard deviation.

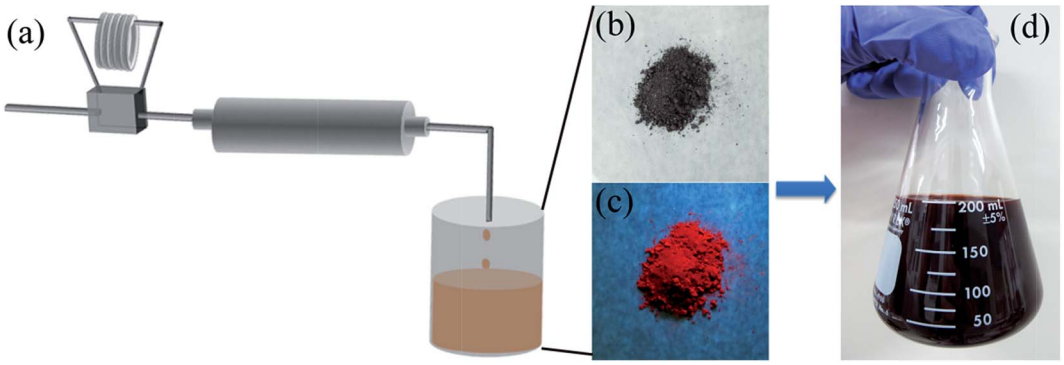

Fig. 7 (a) Schematic picture of our continuous flow system. (b–d) Photographs of 5 g CdSe QDs synthesized by the continuous flow system, under UV excitation, and dispersed in hexane.

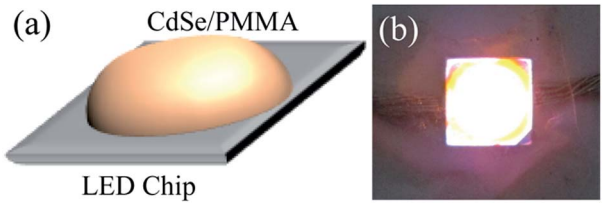

Fig. 8 (a) Schematic diagram and (b) photography of white LEDs fabricated by combination of a blue LED chip with yellow CdSe QDs.

supercritical fluid equipment is feasible. Compared to the conventional batch reactor to produce QDs, the injection rate can be precisely controlled by the HPLC pump, which can reduce the error caused by manual operation. When compared with the microfluidic reactor, the channel to deliver reactants has a higher volume flow rate because of a relatively large diameter (1/8″ i.d.) and the reactor also has a larger volume (10 mL). Therefore, the production rate is superior to the microfluidic reactor (1/16″ i.d.)

The CdSe QDs synthesized by our approach can be used as phosphors in some applications. For example, white LEDs have received considerable attention because of their many advantages over conventional light such as long lifetime and high efficiency.[63] White light can be generated by mixed blue and yellow emission. Therefore, we can simply fabricate white LEDs by combining blue LED chips with yellow CdSe QDs. The photograph of the device is shown in Fig. 8. Furthermore, we have also synthesized other QDs to prove the general applicability of this system. Fig. 9 shows the TEM, HRTEM images, SAED, and XRD patterns of CdS, ZnS, and ZnSe QDs, which were produced by using similar experimental conditions as

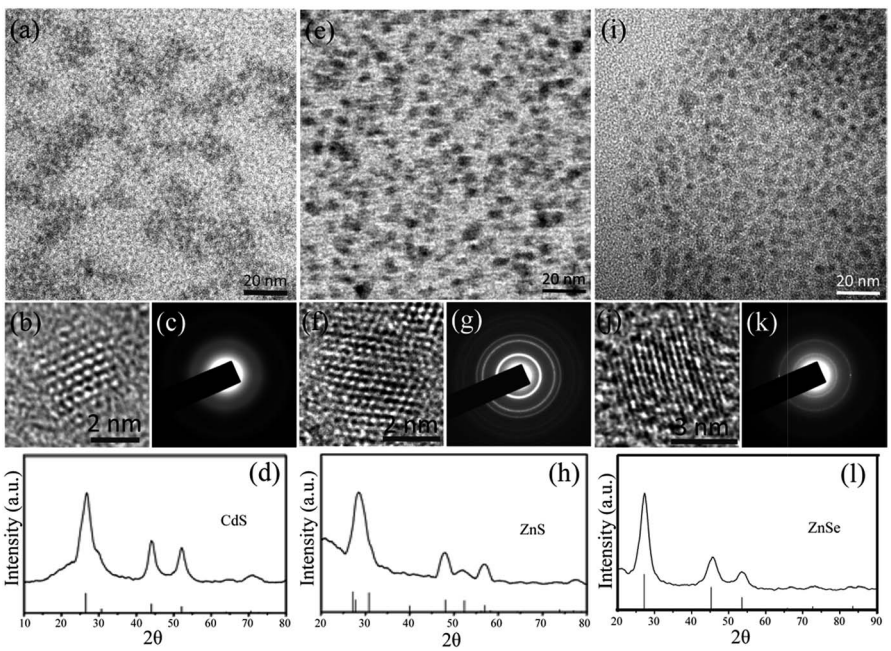

Fig. 9 Different QDs synthesized from hexane-based flow reactors. CdS QDs: (a) TEM, (b) HRTEM, (c) SAED pattern, and (d) XRD pattern. ZnS QDs: (e) TEM, (f) HRTEM, (g) SAED pattern, and (h) XRD pattern. ZnSe QDs: (i) TEM, (j) HRTEM, (k) SAED pattern, and (l) XRD pattern of ZnSe QDs.

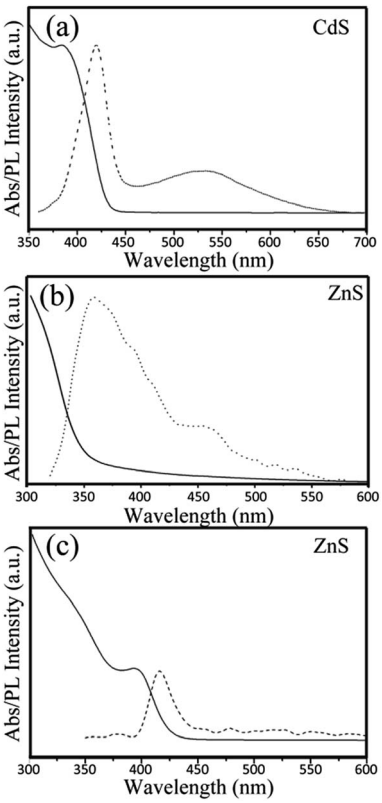

Fig. 10 UV-vis absorption (solid line) and PL spectra (dotted line) of (a) CdS, (b) ZnS, and (c) ZnSe QDs.

described for CdSe QDs. Based on the TEM image, the statistical average diameters for the CdS, ZnS, and ZnSe QDs were about 3.8 nm, 4.3 nm, and 4.6 nm, respectively. Clear lattice planes were observed by HRTEM images, which confirmed the high crystallinity of these nanoparticles. The crystal structures confirmed by SAED and XRD patterns were face centered cubic, hexagonal, and face centered cubic for the CdS, ZnS, and ZnSe, respectively. In addition, the optical properties of these QDs (UV-vis absorption and PL spectra) are shown in Fig. 10. Based on the abovementioned results and the various advantages, we believe that the supercritical equipment has the potential to enable the production of a wide variety of nanomaterials.

Conclusions

In summary, we have demonstrated a generalized and comparatively greener synthetic route for the synthesis of colloidal fluorescing quantum dots under pressurized hexane. First, CdSe QDs as a nanomaterial with sizes ranging between 2.01–5.61 nm, emission wavelengths ranging from 450 nm to 630 nm, and color ranging from green to red can be fabricated by varying the reaction parameters such as temperature and growth time. Second, gram-scale production of 5 g CdSe QDs has been shown by modifying the batch reactor into a continuous reactor with rate production up to 2.5 g h^{-1}. Third, CdS, ZnS, and ZnSe QDs can be synthesized using this supercritical equipment, which indicates that the developed approach has the potential to synthesize other QDs. Finally, compared with the commonly used solvent (high molecular weight) in conventional hot injection or non-injection methods, the high pressure environment allows us to select low molecular weight solvents as reaction medium (greener solvent), having relatively high molecular diffusion (lower viscosity), unlimited reaction temperature, and providing a wide selection of chemical compounds (precursors and ligands). Therefore, this is a flexible and ideal approach for the continuous production of colloidal nanoparticles in large scale and even for industrialization.

Acknowledgements

The authors acknowledge the financial support by the Ministry of Science and Technology of Taiwan (NSC 102-2221-E-007-023-MY3, NSC 102-2221-E-007-090-MY2, NSC 101-2623-E-007-013-IT, and NSC 102-2633-M-007-002), the Ministry of Economic Affairs, Taiwan (101-EC-17-A-09-S1-198), National Tsing Hua University (102N2051E1), and the assistance from Center for Energy and Environmental Research, National Tsing-Hua University.

Notes and references

1 R. Freeman and I. Willner, *Chem. Soc. Rev.*, 2012, **41**, 4067–4085.
2 J. Y. Kim, O. Voznyy, D. Zhitomirsky and E. H. Sargent, *Adv. Mater.*, 2013, **25**, 4986–5010.
3 I. Moreels, K. Lambert, D. Smeets, D. De Muynck, T. Nollet, J. C. Martins, F. Vanhaecke, A. Vantomme, C. Delerue, G. Allan and Z. Hens, *ACS Nano*, 2009, **3**, 3023–3030.
4 L. Wang, H. Wang, Y. Nemoto and Y. Yamauchi, *Chem. Mater.*, 2010, **22**, 2835–2841.
5 H. Ataee-Esfahani, Y. Nemoto, L. Wang and Y. Yamauchi, *Chem. Commun.*, 2011, **47**, 3885–3887.
6 C. X. Guo, S. Huang and X. Lu, *Green Chem.*, 2014, **16**, 2571–2579.
7 P. V. Kamat, *J. Phys. Chem. C*, 2008, **112**, 18737–18753.
8 D. V. Talapin, J. S. Lee, M. V. Kovalenko and E. V. Shevchenko, *Chem. Rev.*, 2010, **110**, 389–458.
9 P. Zrazhevskiy, M. Sena and X. H. Gao, *Chem. Soc. Rev.*, 2010, **39**, 4326–4354.
10 M.-Y. Chiang, S.-H. Chang, C.-Y. Chen, F.-W. Yuan and H.-Y. Tuan, *J. Phys. Chem. C*, 2011, **115**, 1592–1599.
11 S.-H. Chang, M.-Y. Chiang, C.-C. Chiang, F.-W. Yuan, C.-Y. Chen, B.-C. Chiu, T.-L. Kao, C.-H. Laic and H.-Y. Tuan, *Energy Environ. Sci.*, 2011, **4**, 4929–4932.
12 W. Liu, D. B. Mitzi, M. Yuan, A. J. Kellock, S. Jay Chey and O. Gunawan, *Chem. Mater.*, 2010, **22**, 1010–1014.
13 D. Bera, L. Qian, T. K. Tseng and P. H. Holloway, *Materials*, 2010, **3**, 2260–2345.
14 A. J. Nozik, M. C. Beard, J. M. Luther, M. Law, R. J. Ellingson and J. C. Johnson, *Chem. Rev.*, 2010, **110**, 6873–6890.
15 C. B. Murray, D. J. Norris and M. G. Bawendi, *J. Am. Chem. Soc.*, 1993, **115**, 8706–8715.

16 Z. A. Peng and X. G. Peng, *J. Am. Chem. Soc.*, 2001, **123**, 183–184.
17 C. Bullen and P. Mulvaney, *Langmuir*, 2006, **22**, 3007–3013.
18 C. D. Donega, P. Liljeroth and D. Vanmaekelbergh, *Small*, 2005, **1**, 1152–1162.
19 J. Y. Rempel, M. G. Bawendi and K. F. Jensen, *J. Am. Chem. Soc.*, 2009, **131**, 4479–4489.
20 A. C. S. Samia, S. Dayal and C. Burda, *Photochem. Photobiol.*, 2006, **82**, 617–625.
21 D. V. Talapin, A. L. Rogach, A. Kornowski, M. Haase and H. Weller, *Nano Lett.*, 2001, **1**, 207–211.
22 J. van Embden and P. Mulvaney, *Langmuir*, 2005, **21**, 10226–10233.
23 E. M. Chan, R. A. Mathies and A. P. Alivisatos, *Nano Lett.*, 2003, **3**, 199–201.
24 S. G. Kwon and T. Hyeon, *Small*, 2011, **7**, 2685–2702.
25 X. G. Peng, J. Wickham and A. P. Alivisatos, *J. Am. Chem. Soc.*, 1998, **120**, 5343–5344.
26 Y. A. Yang, H. M. Wu, K. R. Williams and Y. C. Cao, *Angew. Chem., Int. Ed.*, 2005, **44**, 6712–6715.
27 J. J. Zhu, O. Palchik, S. G. Chen and A. Gedanken, *J. Phys. Chem. B*, 2000, **104**, 7344–7347.
28 R. K. Capek, K. Lambert, D. Dorfs, P. F. Smet, D. Poelman, A. Eychmuller and Z. Hens, *Chem. Mater.*, 2009, **21**, 1743–1749.
29 J. Ouyang, M. B. Zaman, F. J. Yan, D. Johnston, G. Li, X. Wu, D. Leek, C. I. Ratcliffe, J. A. Ripmeester and K. Yu, *J. Phys. Chem. C*, 2008, **112**, 13805–13811.
30 C. R. Bullen and P. Mulvaney, *Nano Lett.*, 2004, **4**, 2303–2307.
31 J. B. Edel, R. Fortt, J. C. deMello and A. J. deMello, *Chem. Commun.*, 2002, 1136–1137.
32 S. Marre, J. Baek, J. Park, M. G. Bawendi and K. F. Jensen, *JALA*, 2009, **14**, 367–373.
33 S. Marre, J. Park, J. Rempel, J. Guan, M. G. Bawendi and K. F. Jensen, *Adv. Mater.*, 2008, **20**, 4830.
34 J. D. Holmes, D. M. Lyons and K. J. Ziegler, *Chem.–Eur. J.*, 2003, **9**, 2144–2150.
35 S. K. Pahari, T. Adschiri and A. B. Panda, *J. Mater. Chem.*, 2011, **21**, 10377–10383.
36 K. Sue, M. Suzuki, K. Arai, T. Ohashi, H. Ura, K. Matsui, Y. Hakuta, H. Hayashi, M. Watanabe and T. Hiaki, *Green Chem.*, 2006, **8**, 634–638.
37 M. J. Armstrong, A. Panneerselvam, C. O'Regan, M. A. Morris and J. D. Holmes, *J. Mater. Chem. A*, 2013, **1**, 10667–10676.
38 Z. Li, J. F. Godsell, J. P. O'Byrne, N. Petkov, M. A. Morris, S. Roy and J. D. Holmes, *J. Am. Chem. Soc.*, 2010, **132**, 12540–12541.
39 X. G. Ye and C. M. Wai, *J. Chem. Educ.*, 2003, **80**, 198–204.
40 F.-W. Yuan, H.-J. Yang and H.-Y. Tuan, *ACS Nano*, 2012, **11**, 9932–9942.
41 F.-W. Yuan, C.-Y. Wang, G.-A. Li, S.-H. Chang, L.-W. Chu, L.-J. Chen and H.-Y. Tuan, *Nanoscale*, 2013, **5**, 9875–9881.
42 S. H. Xu, C. L. Wang, Q. Y. Xu, R. Q. Li, H. B. Shao, H. S. Zhang, M. Fang, W. Lei and Y. P. Cui, *J. Phys. Chem. C*, 2010, **114**, 14319–14326.
43 R. A. Sheldon, *Green Chem.*, 2005, **7**, 267–278.
44 C. Capello, U. Fischer and K. Hungerbuhler, *Green Chem.*, 2007, **9**, 927–934.
45 A. S. Masadeh, E. S. Bozin, C. L. Farrow, G. Paglia, P. Juhas, S. J. L. Billinge, A. Karkamkar and M. G. Kanatzidis, *Phys. Rev. B: Condens. Matter Mater. Phys.*, 2007, **76**, 115413.
46 Y. Lee, J. R. Choi, K. J. Lee, N. E. Stott and D. Kim, *Nanotechnology*, 2008, **19**, 415604.
47 W. W. Yu, L. H. Qu, W. Z. Guo and X. G. Peng, *Chem. Mater.*, 2003, **15**, 2854–2860.
48 N. Q. Wu, L. Fu, M. Su, M. Aslam, K. C. Wong and V. P. Dravid, *Nano Lett.*, 2004, **4**, 383–386.
49 S. T. Chen, X. L. Zhang, Y. B. Zhao, J. L. Yan and W. H. Tan, *Mater. Lett.*, 2009, **63**, 712–714.
50 W. W. Yu, Y. A. Wang and X. G. Peng, *Chem. Mater.*, 2003, **15**, 4300–4308.
51 J. Chen, J. L. Song, X. W. Sun, W. Q. Deng, C. Y. Jiang, W. Lei, J. H. Huang and R. S. Liu, *Appl. Phys. Lett.*, 2009, **94**, 153115.
52 S. T. Chen, X. L. Zhang, Q. H. Zhang and W. H. Tan, *Nanoscale Res. Lett.*, 2009, **4**, 1159–1165.
53 A. M. Smith, H. W. Duan, M. N. Rhyner, G. Ruan and S. M. Nie, *Phys. Chem. Chem. Phys.*, 2006, **8**, 3895–3903.
54 K. Yu, B. Zaman, S. Singh, D. S. Wang and J. A. Ripmeester, *Chem. Mater.*, 2005, **17**, 2552–2561.
55 P. Reiss, M. Protiere and L. Li, *Small*, 2009, **5**, 154–168.
56 S. Asokan, K. M. Krueger, A. Alkhawaldeh, A. R. Carreon, Z. Z. Mu, V. L. Colvin, N. V. Mantzaris and M. S. Wong, *Nanotechnology*, 2005, **16**, 2000–2011.
57 H. Nakamura, Y. Yamaguchi, M. Miyazaki, H. Maeda, M. Uehara and P. Mulvaney, *Chem. Commun.*, 2002, 2844–2845.
58 K. A. Kozek, K. M. Kozek, W. C. Wu, S. R. Mishra and J. B. Tracy, *Chem. Mater.*, 2013, **25**, 4537–4544.
59 S. E. Lohse, J. R. Eller, S. T. Sivapalan, M. R. Plews and C. J. Murphy, *ACS Nano*, 2013, **7**, 4135–4150.
60 S. Marre and K. F. Jensen, *Chem. Soc. Rev.*, 2010, **39**, 1183–1202.
61 Y. J. Song, J. Hormes and C. S. S. R. Kumar, *Small*, 2008, **4**, 698–711.
62 H. Y. Tuan and B. A. Korgel, *Chem. Mater.*, 2008, **20**, 1239–1241.
63 W. Chung, K. Park, H. J. Yu, J. Kim, B. H. Chun and S. H. Kim, *Opt. Mater.*, 2010, **32**, 515–521.

